



OPEN

An Electrically Switchable Metal-Organic Framework

SUBJECT AREAS:

METAL-ORGANIC
FRAMEWORKS

COORDINATION CHEMISTRY

Carlos A. Fernandez¹, Paul C. Martin¹, Todd Schaeff², Mark E. Bowden³, Praveen K. Thallapally², Liem Dang², Wu Xu¹, Xilin Chen¹ & B. Peter McGrail¹

¹Energy and Environment Directorate, Pacific Northwest National Laboratory, Richland, WA 99352, USA, ²Fundamental & Computational Sciences Directorate, Pacific Northwest National Laboratory, Richland, WA 99352, USA, ³Environmental Molecular Sciences Laboratory, Pacific Northwest National Laboratory, Richland, WA 99352, USA.

Received
14 March 2014Accepted
22 July 2014Published
19 August 2014

Correspondence and requests for materials should be addressed to C.A.F. (carlos.fernandez@pnl.gov); B.P.M. (pete.mcgrail@pnl.gov) or P.K.T. (praveen.thallapally@pnl.gov)

Crystalline metal organic framework (MOF) materials containing interconnected porosity can be chemically modified to promote stimulus-driven (light, magnetic or electric fields) structural transformations that can be used in a number of devices. Innovative research strategies are now focused on understanding the role of chemical bond manipulation to reversibly alter the free volume in such structures of critical importance for electro-catalysis, molecular electronics, energy storage technologies, sensor devices and smart membranes. In this letter, we study the mechanism for which an electrically switchable MOF composed of Cu(TCNQ) (TCNQ = 7,7,8,8-tetracyanoquinodimethane) transitions from a high-resistance state to a conducting state in a reversible fashion by an applied potential. The actual mechanism for this reversible electrical switching is still not understood even though a number of reports are available describing the application of electric-field-induced switching of Cu(TCNQ) in device fabrication.

The tremendous challenges associated with an increased demand for energy and the need to use our natural resources more efficiently and effectively are now widely recognized. Currently, many emerging energy technologies including storage, separation, catalysis and batteries are not able to reach full maturity owing to limitations associated with the less than optimum properties of current materials^{1,2}. Nanostructured organic-inorganic hybrid materials, including crystalline metal organic framework (MOF) architectures, comprise an important class of solid-state materials that could address many of these limitations³⁻¹⁷. However, the potential of hybrid materials to solve energy and environmental needs will remain inherently constrained while manipulation of their chemical functionality and structure continues to be limited to standard pressure and temperature stimulation methods¹⁸⁻²¹. Although not shown in MOF type materials, many polymer materials can undergo phase and volume change when subjected to external stimuli such as electrical field or optical effect irradiation²². For example, gels containing polyacrylamide in a solvent, such as acetone-water, undergo a discrete and reversible volume change when a field is applied. The resulting force on charged sites within the network produces a stress gradient along the electric field. There exists a critical stress below which the gel is swollen and above which the gel collapses^{23,24}. Another example includes an amorphous organometallic block copolymer, which transforms from an ordered lamellar phase to a disordered higher volume phase when the oxidation state of resident iron atom of the ferrocene complex is altered by application of a weak electric field²⁵. Much less is known about synthetic approaches to preparing crystalline MOF's and the mechanisms by which applied electric fields will reversibly drive the volume change. Herein we report for the first time, the mechanism for which a MOF composed of TCNQ can reversibly change shape by virtue of an applied potential.

TCNQ is a well-known acceptor molecule which can be easily reduced with electron donors to form the open shell anion radical TCNQ^{*-}. The single unpaired electron is located mainly on the terminal dicyanomethylene carbon groups. Two polymorphs of Cu(TCNQ) were synthesized as thin films by exposing copper substrates to hot solutions of saturated TCNQ in acetonitrile at different temperatures. Cu(TCNQ) phase I was obtained by immersing a copper substrate at 40°C for 5 h while phase II was obtained by exposing the copper substrate at 80°C for a similar period of time. In addition, Cu(TCNQ) phase I can be completely converted to phase II by extending the reaction time to 24 h at 40°C or if films of Cu(TCNQ) phase I are immersed in a saturated solution of TCNQ at 80°C for approximately 5 h. Briefly, Cu(TCNQ) phase I is a highly distorted tetrahedron where four nitrogen atoms coordinate to one Cu atom with N-Cu-N angles between 92° and 142° (Figure 1, left). The quinoid rings of the TCNQ units are arranged in interplanar stacking at a distance of 3.24 Å, which is smaller than the van

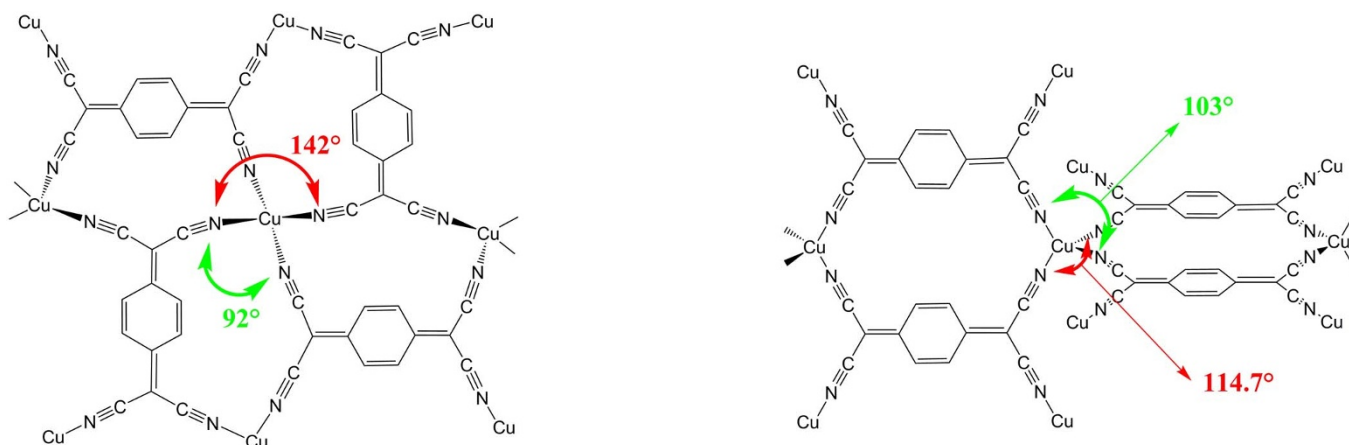


Figure 1 | Cu(TCNQ) phase I (left) and phase II (right). The largest and lowest angles are indicated for both phases. Figure on the right was adapted with permission from Heintz, R. A. et al. *Inorg Chem* **38**, 144–156, (1999). Copyright (1999) American Chemical Society.

der Waals distance of 3.4 Å for carbon atoms. The metal geometry in Cu(TCNQ) phase II is nearly tetrahedral unlike the distorted structure in phase I. The average C-N bond length in phase II is 1.95 Å with N-Cu-N angles around the Cu atom between 103° and 114.7° (Figure 1, right). Adjacent TCNQ ligands are parallel to each other with 6.8 Å being the shortest face-to-face contact between nearest neighbors in the same network (Figure 2, left). Two main differences between Cu(TCNQ) phase I and phase II are responsible for completely different spatial arrangements for the TCNQ ligands in the two structures²⁶. The first difference is the TCNQ relative orientation around Cu atoms. In phase I neighboring TCNQ molecules are rotated 90° with respect to one another (Figure 1, left) while in phase II coplanar TCNQ molecules are oriented in the same direction but in two perpendicular planes (Figure 1, right). The second main difference is the type of interpenetration that they exhibit. The two independent networks in phase I bring the TCNQ molecules together to give a columnar stack with the closest distance being 3.24 Å as shown in Figure 2, right. In contrast, phase II interpenetration does not bring the two independent networks together and the TCNQ rings are “slid” and no π stacking takes place (closest distance 6.8 Å, Figure 2, left)²⁶.

Figure 2 also shows the PXRD patterns for both Phases I and II and the corresponding labeling of the main peaks. Phase II peaks at $2\theta = 9.2^\circ$ corresponds to the (0 0 2) plane which is perpendicular to the N-Cu-N coordination mode. The second highest intensity peak in phase II located at 16.8° corresponds to the (1 0 -1) and (0 1 0). Six more peaks at 22° , 24° , 26° , 28° , 33° and 35° are also labeled in the figure and correspond to planes (0 2 1), (0 2 2), (0 1 3), (0 3 2), (0 3 3) and (0 2 4), respectively. The structure for phase I has only been partially solved (R factor = 23%) and only the lattice parameters and space group are available²⁶. Nevertheless, the pattern show peaks at $2\theta = 9.5$, 16.8° , 17° , 18.2° , 21.2° , 21.8° , 22.5° , 23.8° , 25.2° , 26° , 28.2° and 29° corresponding to (0 0 2), (0 1 0), (1 0 -1), (0 0 4), (1 0 -3), (0 1 3), (1 0 3), (1 1 0), (1 -1 -2), (1 1 3) and (0 1 5) planes. Conductivity measurements on Cu(TCNQ) phase I and phase II indicate that the phases exhibit significantly different charge transport properties showing a value of $4.8 \times 10^{-3} \text{ S cm}^{-1}$ for phase I while phase II shows a conductivity of $5.8 \times 10^{-7} \text{ S cm}^{-1}$. The large difference in conductivity between these two phases can be attributed to the columns of stacked TCNQ molecules formed by interpenetrating networks in Cu(TCNQ) phase I and to the interaction of the d orbitals of the metal with the p orbitals of the cyano bridge^{27,28}. To study the probability of inducing phase transformation between these two Cu(TCNQ) polymorphs, conductivity measurements as a function of applied potential were performed on films of Cu(TCNQ) phase II on a metal/film/metal sandwich structure (details in Methods

Summary). Figure 3 shows a dc current-voltage plot between 0 and 6 V. The cell initially is in an Ohmic high impedance state showing about 100 kOhm in the voltage range of 0–1 V. This is in agreement with the conductivity measurements performed on the insulator Cu(TCNQ) phase II. Figure 3 also shows that the

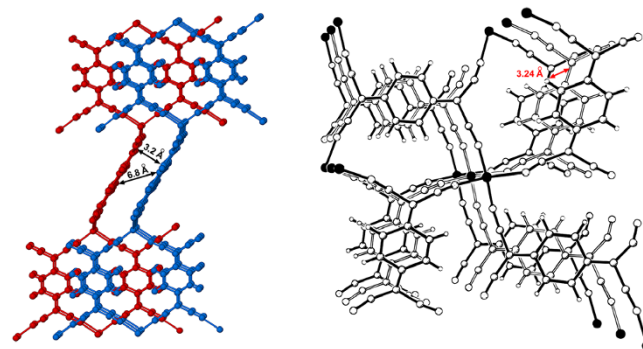
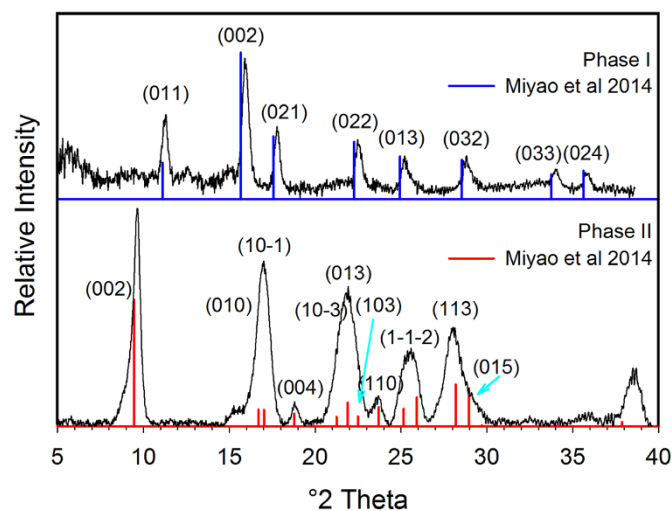


Figure 2 | Top: Powder XRD spectra of TCNQCu active and inactive forms showing peak assignments. Bottom: Interpenetrating networks in phase II (left) and phase I (right). Solid bonds are used for one network and the open bonds for the second network. Interplanar distances shown in both phases. Figure on the right was adapted with permission from Heintz, R. A. et al. *Inorg Chem* **38**, 144–156, (1999). Copyright (1999) American Chemical Society.

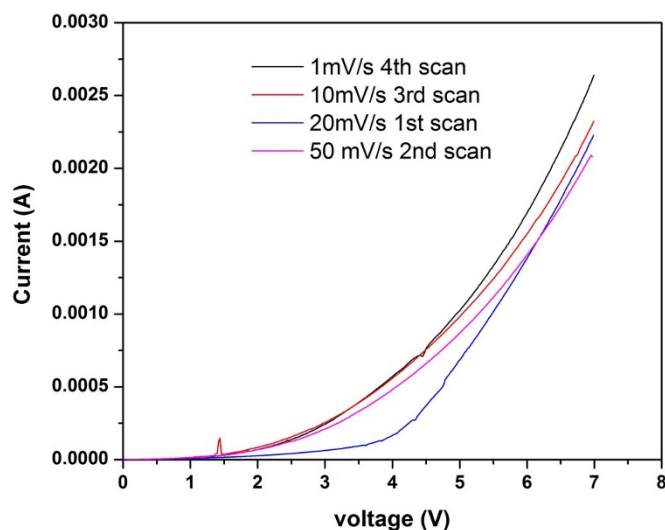


Figure 3 | DC current-voltage plot showing bistable switching in a 10 μm -thick Cu-TCNQ phase II film placed between two electrodes in a sandwich structure. Each new scan was performed after a relaxation period of about a minute.

Cu(TCNQ) film goes from an “off” insulating state to an “on” conducting state at approximately 4.5 V. The impedance of the cell in the voltage range of 4–7 V was estimated in 1,500 Ohm. These results are in agreement with the observations reported by Potember *et al.*²⁹ When the applied potential is removed, the material returns to the initial insulator state. In the following scans, only 2.5 V are needed for the material to show similar current values to the initial scan independently of the scan rate. This could be due to the fact that a small fraction of the conducting phase is still present even after the applied voltage is switched-off. Nevertheless, the figure shows that the “on”/“off” switching process during the following scans is reversible and after removing the applied potential Cu(TCNQ) films seem to return to the original insulator phase (phase II) as confirmed by powder X-ray diffraction (PXRD) spectroscopy. The electrical behavior appeared to be insensitive to air or moisture and was not photo sensitive. In addition, the electrical behavior is fundamentally independent of the direction of the current flow in contrast to what it has been previously reported³⁰. XRD analysis was performed on the as-synthesized bulk as well as films of Cu(TCNQ) phase I and phase II (Figure 2). Each phase shows identical patterns as either films or powder samples. The difference in the XRD spectra between both phases is clearly evident in Figure 2. In addition, both materials show stability against moisture and air as evidenced by the identical patterns after several weeks of films exposure to room temperature and humidity (20% RH).

Switching mechanistic studies on Cu(TCNQ) have been carried out by Potember, Heintz and others. Potember *et al.*²⁹, suggested that the electrical switching might be the result of a phase transition taking place by the formation of mixed-valence species or what scientists call valence-controlled semiconducting properties. Later on, although not proven, Heintz *et al.*²⁶ suggested that the electronic switching could be due to a phase transition between a 3D structure that does not allow for TCNQ⁻ stacking to a phase that brings parallel TCNQ radicals into close proximity. Other groups highlight the importance of the interface to the electrodes (particularly when using Aluminum electrodes) for the resistive switching effect^{28,31–33}. The model proposed by these groups states that a thin interfacial aluminum oxide layer at the Al electrode plays a decisive role. This model was supplemented by additional experiments that indicate that the switching effect in Cu(TCNQ) thin film devices could be a Cu ion based electrochemical effect, i.e., the devices could be described as electrochemical metallization cells, where the aluminum oxide repre-

sents the electrolyte. They attribute the Cu(TCNQ) layer to simply act as a spacer, which possibly stabilizes the reversible switching by acting as a Cu ion buffer.

To gain insight on the electrical switching mechanism, and more importantly, determine if a structural transformation on Cu(TCNQ) plays a role on the electrical switching of Cu(TCNQ) film materials we performed *in operando* X-ray diffraction (XRD) as a function of applied potential. The dynamics of the possible structural transition on Cu(TCNQ) from a high impedance state (phase II) to a low impedance state at increasing applied potentials were studied using a state-of-the-art system. The system was used to collect XRD patterns on a Cu(TCNQ) phase II film at increasingly applied voltages between 0 V and 10 V. Figure 4 (right) shows a summary of the XRD patterns of Cu(TCNQ), both phase I and Phase II, as well as a function of applied DC voltage, including the current intensity measured at each potential value. For reference, a diffraction pattern collected from Cu(TCNQ) phase I film is also provided and closely matches the structural data reported by Miyao *et al.*³⁴ Indexing of both diffraction patterns were based on published cell parameters²⁶.

Initially, Cu(TCNQ) film shows the pattern of the “off” state (phase II) at 0 V³⁴. The most intense reflection, positioned at $9.60^\circ 2\theta$ corresponds to the (0 0 2) plane. Subsequent reflections positioned at higher 2θ values are less intense and appear broader in comparison (Figure 4). Following application of voltage (1.5, 3 and 5 V) to the phase II sample, the observed reflections simultaneously shifted to higher 2θ with an incremental 2θ difference at higher 2θ . For example, the high intensity peak at $9.2^\circ 2\theta$ in Phase II (0 0 2) plane, which is perpendicular to the N-Cu-N coordination mode, shifts from 9.2° to $10.3^\circ 2\theta$ (by 1.1°). The second highest intensity peak in phase II located at $16.8^\circ 2\theta$ corresponds to the (1 0 -1) and (0 1 0) in phase II and shifts from 16.8° to $18.3^\circ 2\theta$ (by 1.5°). This trend continues with peak shifts of nearly 3° (from 27.8° to 30.5°) at higher 2θ . More importantly, the XRD pattern for these intermediate structures are not consistent with a sample displacement or misalignment in the XRD unit. These observations indeed corresponded to a reduction of all three lattice dimensions²⁶, which decreased further with increasing voltage as it is clearly shown in Figure 5. The decreased (002) intensity suggests a distortion of the structure such that atoms, and especially the heavier Cu atoms, are no longer aligned on planes parallel to (001). For example, alternate TCNQ ligands could be displaced in positive and negative directions along *c* and/or rotated about the two aligned C=C double bonds to minimize steric effects in the smaller unit cell. The distortion would result in deviation from the tetrahedral symmetry at the Cu positions resulting in a greater overlap between the hybrid sp orbitals of the cyanide functionalities and the Π system of the benzene rings. The increase observed in electric conductivity of a film of Phase II is the result of this phenomenon as shown in Figures 3 and 4. When applying 6 V, the current measured increases from 6 mA to 9 mA. As importantly, at this point major changes in the XRD pattern of the distorted Phase II, which from now on we call *phase III*, are observed and reflections corresponding to the phase I structure [planes (0 0 2), (0 2 1), (0 2 2) and (0 1 3)] appear as indicated in Figure 4. This represents strong evidence that at these high voltages a fraction of Cu(TCNQ) *phase III* is converting to phase I and both phases coexist as long as this potential is applied. Partial transition from *phase III* to phase I requires bond breakage, framework rearrangement and formation of new Cu-N coordination bonds which does not occur at 3 V and 5 V. It is important to note that the coordination bond energy for Cu-N is in the order of 250 KJ/mol. Then, assuming a potential of 9 V applied for 60 sec (which was the time required to get a spectrum) to 5 mg of Cu(TCNQ) phase II film, the energy provided to the film is 3.2 J or approximately 170 KJ/mol of Cu(TCNQ) *phase III*²⁶. This energy is comparable to the coordination bond energy for Cu-N and seemingly enough to produce some Cu-N coordination bond breaking and reorganization of the structure, including Cu-N bond

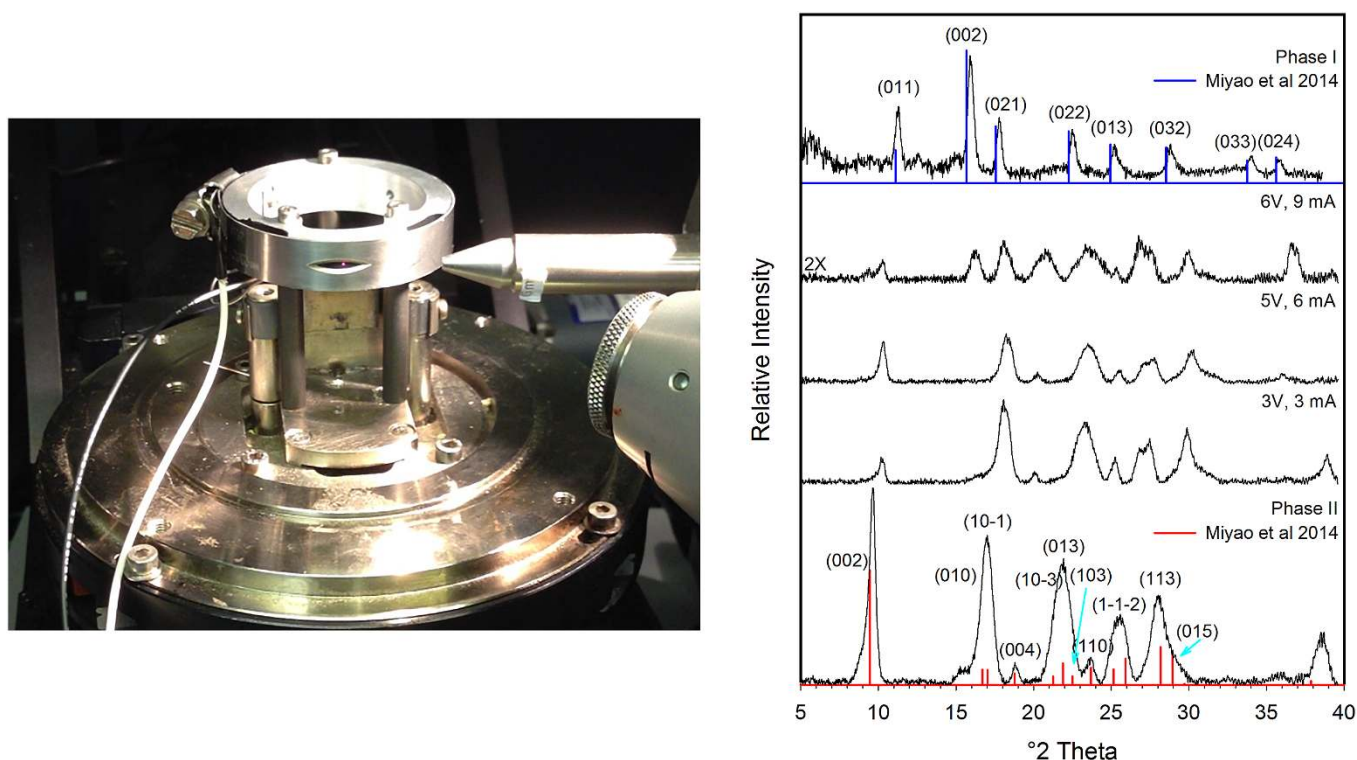


Figure 4 | Left: System constructed in house for in-situ XRD spectrometry vs applied potential to study the kinetics of structural transformations on electro-active materials. Right: XRD spectra of CuTCNQ as a function of voltage showing the reflection planes for both phases I and II.

formation which can be noticeable in the XRD spectrum. Therefore, transition from Cu(TCNQ) phase III to conducting Cu(TCNQ) phase I is possible and it was indeed observed when applying 6 V to the sample. What is surprising is the fact that when applying 3 V (3 mA) and 5 V (6 mA) which corresponds to energy values of 28 KJ/mol and 95 KJ/mol partial reorganization of Cu(TCNQ) phase II to phase I was not observed. Instead, a potential rotation of TCNQ planes around the metal center maybe occurring with the associated increase in conductivity indicating that the material is going from the high-resistance tetrahedral arrangement phase II to a low-resistance structural arrangement *phase III* (Figure 4). Based on this evidence, it is hypothesized that at potentials as low as 3 V the TCNQ ligands at either side of the coordinating metal in phase II may slowly rotate around the metal coordination center until all the aromatic organic moieties form a *nearly* same-plane cyano sp/π

conjugated system (“on” state) that has a conductivity orders of magnitude higher than the “off” form (Figure 6). Although steric impediment would disallow the possibility of having all TCNQ ligands and coordination Cu in one single plane, a *nearly* in-plane π conjugated system together with the stacking of parallel TCNQ molecules into close proximity may play a key role in the conductivity increase of the new *phase III* form of Cu(TCNQ). At larger applied DC potentials (6 V, 9 mA) a structural transition from Cu(TCNQ) phase III to phase I occurs as described above.

Decreasing the voltage shows a decrease in the measured current while, at low enough voltages, the XRD pattern returns to the original “in-active” state (phase II) pattern. The results prove that the “on”/“off” structural transitions are reversible in agreement with the DC current-voltage plots of Figure 3.

Given the fact that this hypothetical new “phase III” only exists upon applying a potential between 2.5 V and 5 V, it is difficult to obtain the exact crystalline structure of the material. Nevertheless, evidence is shown that a new semiconducting phase (Figure 6) is generated where possibly all three structural characteristics, i.e. same plane π conjugated system, interaction of the d orbitals of the metal with the sp orbitals of the cyano bridge, and π - π coupling (stacking of parallel TCNQ molecules) are taking place upon applying a potential on high-resistance films of Cu(TCNQ) phase II. The results of this work demonstrate that, additionally to the reported Cu ion-based electrochemical effect, two reversible structural transitions seem to take place. At low enough voltages a distortion occur where atoms, especially the heavier Cu atoms, are no longer aligned on planes parallel to (0 0 1) which results in deviation from the tetrahedral symmetry and greater overlap between the hybrid sp orbitals of the cyanide functionalities and the Π system of the benzene rings (phase III in Figure 6). At higher potentials, a greater change in the XRD pattern is observed and a structural transition from the proposed conducting phase III to conducting phase I is evidenced. In this second transition bonds breaking and formation takes place on Cu(TCNQ) further contributing to the electrical switching processes.

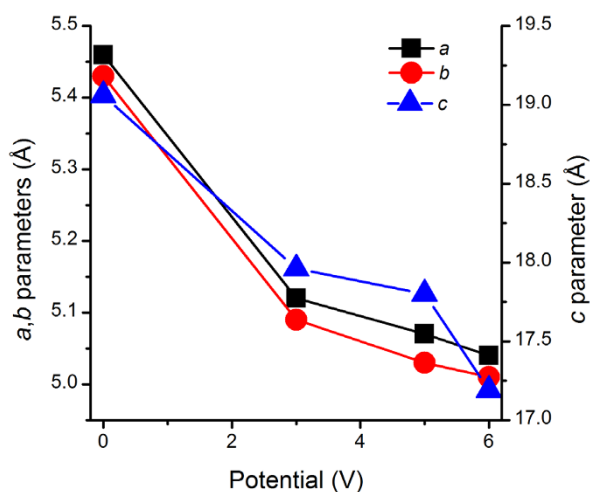


Figure 5 | Phase II cell parameters as a function of applied potential.

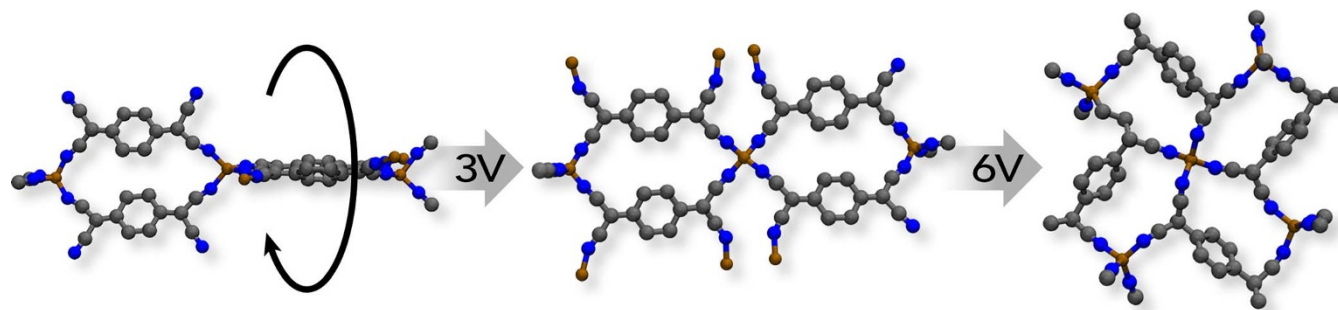


Figure 6 | Single crystal structure of TCNQCu “off” state phase II (left) transitioning to a proposed new “on” state phase III (center) at 3 V followed by a transition to phase I at 6 V as described in the main text.

These results have significant implications in the design and fabrication of new functional materials for electronic and magnetic devices. For example, high surface area switchable porous MOFs that could be regenerated electrically provide a new electric power driven thermodynamic cycle upon which a highly efficient heat pump for electric vehicles can be developed²¹. Work toward this goal is ongoing.

Methods Summary

Bulk synthesis of Cu(TCNQ) phase I was performed following a reported synthesis with some modification as follow²⁹. Equimolar quantities of CuI and TCNQ were reacted in acetonitrile at 60 °C for a few minutes while phase II was obtained by continuing the reaction under identical conditions for three days.

Conductivity measurements on pellets. Conductivity analysis on pellets was performed at room temperature by using a Solartron Potentiostat/Galvanostat SI1287A coupled with a Solartron Frequency Response Analyzer SI1255B. Silver paste was applied on both sides of the pellet to reduce the interface resistance between the pellet and the current collector.

Current/voltage measurements. A thin aluminum foil was pressed against a Cu(TCNQ) phase II film deposited on Cu as another current collector (counter electrode). Electrical connection was made to the copper and aluminum electrodes by solder or mechanical crimping. The surface area of the metal/film/metal sandwich structure was approximately 1 cm². Scan rates from 1 mV/s to 50 mV/s were used.

In situ PXRD as a function of potential. The device was designed and constructed in house to measure XRD patterns on electro-active materials deposited on a given substrate. The electrical connections were made to a worm drive clamp, carefully tightened over the deposited materials, and a wire crimped to a freshly abraded surface at the end of the metallic substrate (Figure 4). The surface of the sandwich structure is tangential to the direction of the x-ray beam and has a small slit which extends in the same direction of the beam and exposes a small area of the porous material to the beam. The detector is located on the other side of the system forming nearly 180 degrees with the sample and the Cu source. Both aluminum electrodes are connected to the positive or negative terminal of a potentiometer to apply and read voltage and current.

1. Furukawa, H., Cordova, K. E., O’Keeffe, M. & Yaghi, O. M. The chemistry and applications of metal-organic frameworks. *Science* **341**, 1230444, doi:10.1126/science.1230444 (2013).
2. Zhou, H. C., Long, J. R. & Yaghi, O. M. Introduction to metal-organic frameworks. *Chem Rev* **112**, 673–674, doi:10.1021/cr300014x (2012).
3. Carbonera, C., Dei, A., Letard, J. F., Sangregorio, C. & Sorace, L. Thermally and light-induced valence tautomeric transition in a dinuclear cobalt-tetraoxolene complex. *Angew Chemie* **43**, 3136–3138, doi:10.1002/anie.200453944 (2004).
4. Halder, G. J., Kepert, C. J., Moubaraki, B., Murray, K. S. & Cashion, J. D. Guest-dependent spin crossover in a nanoporous molecular framework material. *Science* **298**, 1762–1765, doi:10.1126/science.1075948 (2002).
5. MasPOCH, D., Ruiz-Molina, D. & Veciana, J. Old materials with new tricks: multifunctional open-framework materials. *Chem Soc rev* **36**, 770–818, doi:10.1039/b501600m (2007).
6. Metzger, R. M. & Torrance, J. B. Role of the Madelung Energy in the Neutral Ionic Phase-Transition of Tetrathiafulvalene Chloranil. *J Am Chem Soc* **107**, 117–121, doi:10.1021/Ja00287a021 (1985).
7. Okamura, H. *et al.* Infrared study of spin crossover Fe-picolyamine complex. *J Phys Soc Jpn* **73**, 1355–1361, doi:10.1143/Jpsj.73.1355 (2004).
8. Okamura, H. *et al.* Photoinduced spin crossover in a Fe-picolyamine complex: A far-infrared study on single crystals. *Phys Rev B* **72**, doi:Artn 073108 Doi 10.1103/Physrevb.72.073108 (2005).

9. Kato, R., Kobayashi, H. & Kobayashi, A. Crystal and Electronic-Structures of Conductive Anion-Radical Salts, (2,5-R1,R2-Dcnqi)2cu (Dcnqi = N,N’-Dicyanoquinonediimine – R1, R2 = CH3, CH3O, Cl, Br). *J Am Chem Soc* **111**, 5224–5232, doi:10.1021/Ja00196a032 (1989).
10. Biswal, B. P., Pandaa, T. & Banerjee, R. Solution mediated phase transformation (RHO to SOD) in porous Co-imidazole based zeolitic frameworks with high water stability. *Chem Comm* **48** (2012).
11. vonSchutz, J. U., Gomez, D., Schmitt, H. & Wachtel, H. Conductivity without spin-signal, spin signal without conductivity switchable radical ion salts of deuterated Cu(DCNQI)(2). *Synthetic Met* **86**, 2095–2096, doi:10.1016/S0379-6779(97)81044-2 (1997).
12. Banerjee, R. *et al.* Control of Pore Size and Functionality in Isorecticular Zeolitic Imidazole Frameworks and their Carbon Dioxide Selective Capture Properties. *J Am. Chem. Soc.* **101**, 3875–3877 (2009).
13. Fernandez, C. A., Thallapally, P. K. & McGrail, B. P. Insights into the Temperature-Dependent “Breathing” of a Flexible Fluorinated Metal–Organic Framework. *ChemPhysChem* **13**, 3275–3281 (2012). DOI: 10.1002/cphc.201200243.
14. Ota, A., Yamochi, H. & Saito, G. A novel metal-insulator phase transition observed in (EDO-TTF)(2)PF6. *J Mater Chem* **12**, 2600–2602, doi:10.1039/B206293c (2002).
15. Chollet, M. *et al.* Gigantic photoresponse in 1/4-filled-band organic salt (EDO-TTF)(2)PF6. *Science* **307**, 86–89, doi:10.1126/science.1105067 (2005).
16. Fernandez, C. A. *et al.* Gas-Induced Expansion and Contraction of a Fluorinated Metal–Organic Framework. *Cryst. Growth Des.* **10**, 1037–1039 (2010) doi: 10.1021/cg9014948.
17. Serre, C. *et al.* Role of Solvent-Host Interactions That Lead to Very Large Swelling of Hybrid Frameworks. *Science* **315**, 1828–1831 (2007), doi: 0.1126/science.1137975.
18. Serre, C. *et al.* Role of solvent-host interactions that lead to very large swelling of hybrid frameworks. *Science* **315**, 1828–1831, doi:10.1126/science.1137975 (2007).
19. Stuart, M. A. *et al.* Emerging applications of stimuli-responsive polymer materials. *Nat Mater* **9**, 101–113, doi:10.1038/nmat2614 (2010).
20. Theato, P., Sumerlin, B. S., O’Reilly, R. K. & Epps, T. H., 3rd. Stimuli responsive materials. *Chem Soc rev* **42**, 7055–7056, doi:10.1039/c3cs90057f (2013).
21. McGrail, B. P., Thallapally, P. K. & Xu, W., inventors. Battelle Memorial Institute, assignee. Methods for Associating or Dissociating Guest Materials with a Metal Organic Framework, Systems for Associating or Dissociating Guest Materials within a Series of Metal Organic Frameworks, and Gas Separation Assemblies. United States patent US 8,425,662. 2013 Apr 23.
22. Lyndon, R. *et al.* Dynamic photo-switching in metal-organic frameworks as a route to low-energy carbon dioxide capture and release. *Angew Chemie* **52**, 3695–3698, doi:10.1002/anie.201206359 (2013).
23. Alvaro, M., Ferrer, B., Garcia, H. & Rey, F. Photochemical modification of the surface area and tortuosity of a trans-1,2-bis(4-pyridyl)ethylene periodic mesoporous MCM organosilica. *Chem Comm* 2012–2013 (2002).
24. Batail, P., Laplaca, S. J., Mayerle, J. J. & Torrance, J. B. Structural Characterization of the Neutral-Ionic Phase-Transition in Tetrathiafulvalene-Chloranil - Evidence for C-H...O Hydrogen-Bonding. *J Am Chem Soc* **103**, 951–953, doi:10.1021/Ja00394a045 (1981).
25. Tanaka, T., Nishio, I., Sun, S. T. & Ueno-Nishio, S. Collapse of gels in an electric field. *Science* **218**, 467–469, doi:10.1126/science.218.4571.467 (1982).
26. Heintz, R. A. *et al.* New insight into the nature of Cu(TCNQ): Solution routes to two distinct polymorphs and their relationship to crystalline films that display bistableswitching behavior. *Inorg Chem* **38**, 144–156 (1999).
27. Aumuller, A. *et al.* Mehrstufige reversible Redoxsysteme, LV. Kristallstruktur des CT-Komplexes 2,5-Me2-DCNQI/TTF aus N,N’-Dicyan-2,5-dimethyl-1,4-benzochinondiimin und Tetrathiafulvalen sowie des Acceptors 2,5-Me2-DCNQI. *Chem. Ber.* **124**, 1991 (2001).
28. Sinzger, K. *et al.* The organic metal (Me2-DCNQI)2Cu: Dramatic changes in solid-state properties and crystal structure due to secondary deuterium effects. *J. Am. Chem. Soc.* **115**, 7696 (1993).



29. Potember, R. S., Poehler, T. O. & Cowan, D. O. Electrical switching and memory phenomena in Cu-TCNQ thin films. *Appl. Phys. Lett.* **34**, 15 (1979).
30. Kever, T., Klopstra, B., Boettger, U. & Waser, R. *IEEE NVMTS Proceedings 2006*, pages 116–119 (2006).
31. Colle, M., Buchel, M. & de Leeuw, D. M. Switching and filamentary conduction in non-volatile organic memories. *Org Electron*, UK, **7**, 305–12 (2006).
32. Oyamada, T., Tanaka, H., Matsushige, K., Sasabe, H. & Adachi, C. Switching effect in Cu:TCNQ charge transfer-complex thin films by vacuum codeposition. *App Phys Lett* **83**, 1252–4 (2003).
33. Hoagland, J. J., Wang, X. D. & Hipps, K. W. Characterization of Cu-Cu-TCNQM Devices Using Scanning Electron Microscopy and Scanning Tunneling Microscopy. *Chem Mat* **5**, 54–60 (1993).
34. Miyao, K., Funabiki, A., Takahashi, K., Mochida, T. & Uruichib, M. Reversible iodine absorption of nonporous coordination polymer Cu(TCNQ). *New J. Chem.* **38**, 739–743 (2014).

Acknowledgments

This work was performed at Pacific Northwest National Laboratory (PNNL) and was supported by the U.S. Department of Energy, ARPA-E thermal energy storage through High Energy Advanced Thermal Storage (HEATS) program. We thank Dr. James Klausner for programmatic support and helpful discussions throughout the project life cycle. PNNL is operated by Battelle for DOE under contract DE-AC05-76RL01830.

Author contributions

C.A.F. wrote the main manuscript and performed the synthesis and characterization including design of materials and methods, P.C.M. designed and constructed the XRD cell for XRD spectra as a function of potential studies, T.S., M.B. and L.D. performed the complete structures analysis and contributed to the writing of this section of the manuscript, P.K.T. is a project task lead and contributed to materials design and writing the manuscript, W.X. and X.C. performed measurements of current vs. potential for a number of samples and wrote part of the manuscript as well, B.P.M. is the project manager and the lead on this study who also contributed to the writing of the manuscript. All authors reviewed the manuscript.

Additional information

Competing financial interests: The authors declare no competing financial interests.

How to cite this article: Fernandez, C.A. *et al.* An Electrically Switchable Metal-Organic Framework. *Sci. Rep.* **4**, 6114; DOI:10.1038/srep06114 (2014).



This work is licensed under a Creative Commons Attribution-NonCommercial-ShareAlike 4.0 International License. The images or other third party material in this article are included in the article's Creative Commons license, unless indicated otherwise in the credit line; if the material is not included under the Creative Commons license, users will need to obtain permission from the license holder in order to reproduce the material. To view a copy of this license, visit <http://creativecommons.org/licenses/by-nc-sa/4.0/>